Effect of moisture condensation on vapour transmission through porous membranes

Ariana Khakpour ⓘ**, Michael Gibbons** ⓘ
and Sanjeev Chandra

Abstract

Porous membranes find natural application in various fields and industries. Water condensation on membranes can block pores, reduce vapour transmissibility, and diminish the porous membranes' performance. This research investigates the rate of water vapour transmission through microporous nylon and nanofibrous Gore-Tex membranes. Testing consisted of placing the membrane at the intersection of two chambers with varied initial humidity conditions. One compartment is initially set to a high $(R_h = 95\%)$ water vapour concentration and the other low $(R_h = <10\%)$, with changes in humidity recorded as a function of time. The impact of pore blockage was explored by pre-wetting the membranes with water or interposing glycerine onto the membrane pores before testing. Pore blockage was measured using image analysis for the nylon membrane. The mass flow rate of water vapour $(\dot{m}_v)$ diffusing through a porous membrane is proportional to both its area (A) and the difference in vapour concentration across its two faces (ΔC), such that $\dot{m}_v = KA\Delta C$ where K is defined as the moisture diffusion coefficient. Correlations are presented for the variation of K as a function of ΔC. Liquid contamination on the porous membrane has been shown to reduce the moisture diffusion rate through the membrane due to pore blockage and the subsequent reduced open area available for vapour diffusion. Water evaporation from the membrane's surface was observed to add to the mass of vapour diffusing through the membrane. A model was developed to predict the effect of membrane wetting on vapour diffusion and showed good agreement with experimental data.

Department of Mechanical and Industrial Engineering, University of Toronto, Toronto, Canada

Corresponding author:
Ariana Khakpour, Department of Mechanical and Industrial Engineering, University of Toronto, 27 King's College Circle, Toronto, Ontario M5S 1A1, Canada.
Email: a.khakpour@mail.utoronto.ca

Introduction

Cotton garments, which are constructed from natural fibres, aid body temperature regulation due to the fabric's pores, which allow moisture evaporating from the skin to leave the clothing envelope without significant resistance [1]. More recently, breathable, thin synthetic materials such as Gore-Tex have been developed. Gore-Tex consists of nanoporous layers of expanded polytetrafluoroethylene that allow air and water vapour to pass through them. Such materials have traditionally been used to make windproof clothing and are now being tested in other applications such as building construction [2].

A growing application of porous membranes is in pressure-relief vents for electronic enclosures, such as LED lights or CCTV cameras. These devices generate large amounts of heat and can not be hermetically sealed due to the internal pressures that develop within their enclosures during operation. Instead, they are equipped with porous membrane vents that allow air and water vapour to pass through while blocking dust particles and water droplets [3]. However, if sufficient water vapour accumulates inside the enclosure and there is a large enough temperature drop, that liquid will condense [4,5] on the electronic components, possibly causing damage. To correctly design these devices, it is essential to know the rate at which moisture diffuses through these porous membranes.

Moisture permeability is a physical property of fabrics and nanofibrous filters that depends on their porosity [6], which may vary depending on operating or environmental conditions. Mechanical stresses, such as those generated by stretching, can change the pressure drop of air flowing through porous filters [7,8]. Temperature changes may also produce mechanical stresses that alter pore geometry [9]. More importantly, in urban environments, solid particle pollutants can accumulate on filters blocking their pores over time [10]. The reduced number of pores in a contaminated porous membrane results in an increased pressure drop across its structure [11], increasing its resistance to vapour transmission. Additionally, increased fluid velocity due to wind can alter the convective mass transfer to the porous membrane, altering the moisture permeation rate [12,13].

Wetting of a porous membrane due to water impingement or condensation can also impact its permeability. The swelling of hygroscopic cotton fibres has been shown to reduce vapour transmission [14]. Water condensation on fabrics has been shown to influence their moisture transmissivity [15,16], but the mechanism behind this is not well understood. Depending on the temperature and ambient humidity conditions, the pores in a membrane could either act as moisture sink, where the vapour condenses, or a source, where accumulated water evaporates and adds to

that diffusing through it [17]. Farnworth et al. [18] observed a significant fluctuation in Gore-Tex's water vapour resistance as temperature and relative humidity were varied.

The work is the first to investigate the impact of pore blockage and water condensation on the water vapour transmissivity of hydrophobic microporous and nanofibrous membranes. Testing consisted of placing the membrane at the intersection of two chambers with varied initial humidity conditions. One compartment is initially set to a high water vapour concentration and the other low, with changes in humidity recorded as a function of time. The impact of pore blockage was explored by pre-wetting the membranes with water or interposing glycerine onto the membrane pores before testing. Pore blockage was measured using image analysis for the nylon membrane.

Experimental setup and data processing methodology

Experimental apparatus

An experimental facility was constructed to investigate the moisture transmission behaviour through porous membranes. The test setup is shown in Figure 1. It consists of a dual-chamber apparatus and an air supply unit to study moisture flow from a moist environment chamber into a dry environment chamber through the porous membrane.

Dual-chamber apparatus. A test chamber was built consisting of two compartments, one "moist " in which the relative humidity (R_h) was maintained above 95% and the other "dry" in which the initial relative humidity was below 10%. The porous membrane separated the two compartments, and changes in humidity on both sides were measured as water vapour diffused from the moist side to the dry side. Figure 1 shows a cubic chamber ($8 \times 8 \times 8$ in.^{3}) made from $1/2$ in. thick, clear polycarbonate sheets (McMaster-Carr®, U.S), divided into two air-tight compartments by a vertical plate. One wall of each compartment was a removable plate to allow access to the respective internal chambers. Each chamber was equipped with a high accuracy temperature and relative humidity sensor (P/N: HX94B, OMEGA Engineering®, U.S) . The two chambers were connected by a $1^1/4$ in. diameter hose fitting (McMaster-Carr®, U.S.) installed in the center of the plate separating the two compartments.

The test membrane was installed across the opening of this fitting with a steel washer that pressed the membrane's circumference against a flange, as shown in Figure 2. Prior to testing, the two chambers are isolated from each other by a flat magnetic lid with an attached silicone gasket that covered the fabric membrane (see Figure 2), blocking the linking hole until the desired humidity conditions are reached. The magnetic lid does not directly contact the fabric membrane to avoid contamination. A linear solenoid (P/N: 7723K5, McMaster-Carr®, U.S) connected
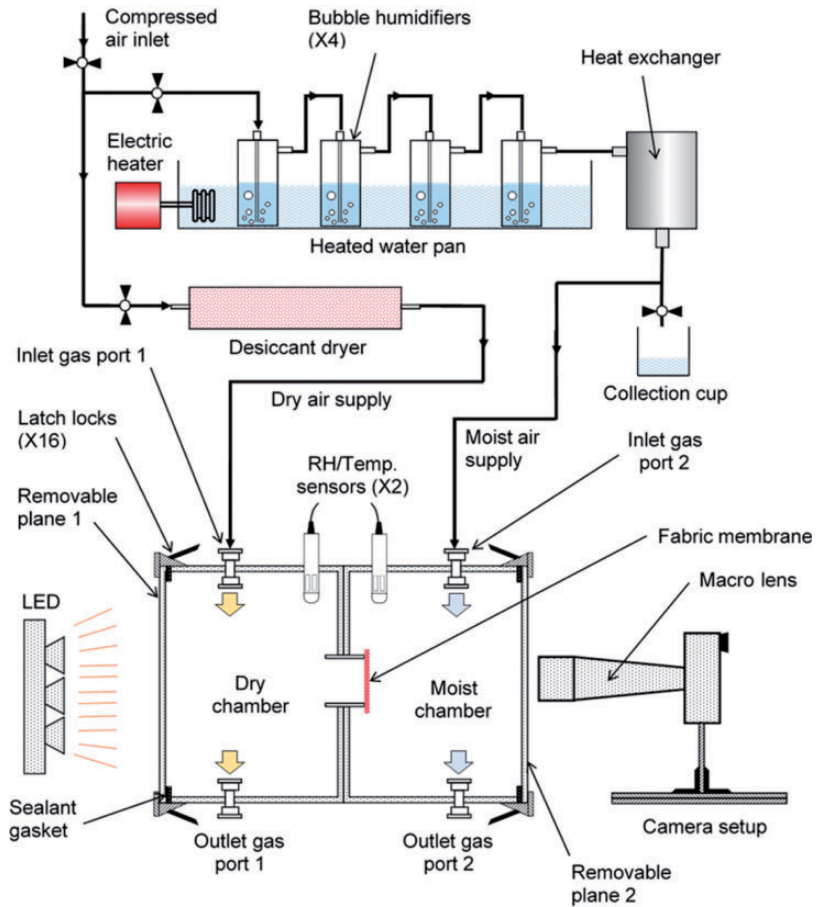
Figure 1. Schematic diagram of the experimental apparatus.

to the magnetic lid was used to remove it, exposing the porous membrane at the start of testing.

Air supply unit. A description of the air supply lines is shown in Figure 1. Air with low water vapour concentration ($R_h < 10\%$) was supplied to the dry chamber by passing air through a cylinder filled with $CaSO_4$ desiccant (W.A. HAMMOND DRIERITE CO. LTD, U.S) . Moist air was established by flowing air through a series of four bubble humidifiers (SALTER LABS®, U.S) immersed in a heated water pan (McMaster-Carr®, U.S). The air was cooled back to room temperature by passing it through a custom-built cold-bath heat exchanger consisting of a copper coil placed in a water bath and any remaining liquid droplets removed by passing it through a sharp bend in a T-fitting that was periodically drained.
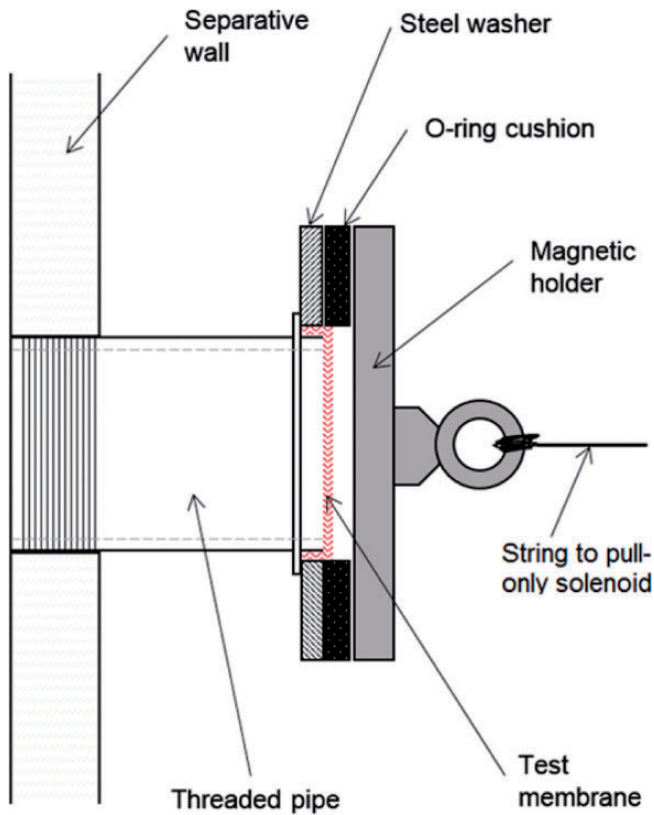
Figure 2. Schematic diagram of the vent sealing mechanism. With the activation of a toggle switch, the magnetic lid is pulled away, exposing the test membrane.

The liquid-free vapour ($R_h \geq 95\%$, T $\approx 22\,°C$) was then delivered to the moist chamber.

Selected porous membranes. This study investigated two different fabric membranes: a microporous nylon membrane and a nanoporous Gore-Tex membrane. Their specifications are listed in Table 1 [19,20]. An SEM (Scanning Electron Microscope) image of the nylon membrane is given in Figure 3(a), and an SEM image of the Gore-Tex membrane is shown in Figure 3(b). It can be seen from Figure 3(b) that the Gore-Tex membrane is constructed of multiple layers of expanded PTFE with fibres in each layer oriented randomly.

Experimental procedure

Test procedure. Before starting the experiment, the two chambers were isolated by the magnetic lid (see Figure 2) covering the porous membrane. The desired relative

Table 1. Technical specifications of the tested fabric membrane.

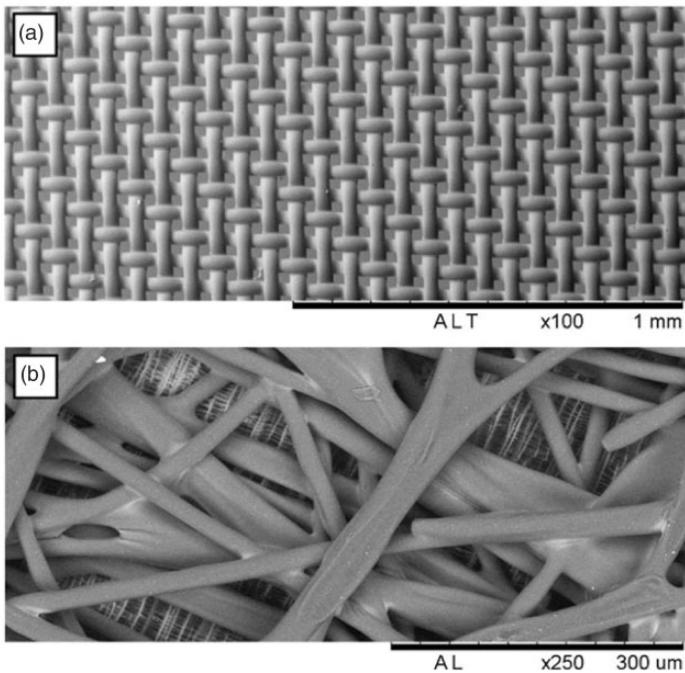|	Microporous membrane [19]	Nanoporous membrane [20]
Fibre material	Nylon	Expanded PTFE (ePTFE)
Structure	Single-layer woven grid	Random 3D
Pore area	1265 μm^2	$\approx$ 280 nm^2
Porosity ratio	28%	N/A
Thickness	0.033 mm	0.26 mm
Surface area	531.5 mm^2	122.7 mm^2
Supplier	McMASTER-CARR®	W. L. Gore & Associates, Inc.®
Part No.	9318T25	VE8 series

Figure 3. (a) SEM view of the nylon membrane under 100× magnification. (b) SEM view of the Gore-Tex membrane with a 250× magnification. The Gore-Tex membrane has a nano-porous structured mesh underneath a larger, randomly structured layer.

humidity conditions in each chamber were established by supplying moist ($R_h = 95\%$) and dry air ($R_h = <10\%$) to each, after which the air supply was turned off and the connecting lines to the chambers were closed. At the start of the experiment, the magnetic lid was removed, and the porous membrane was

exposed. There was no airflow in the chambers during the experiment, and the internal pressure remained constant and in equilibrium with the ambient air pressure. A small water container was placed in the high humidity chamber before testing to maintain saturation conditions. Data was continually recorded as the moisture diffused into the dry chamber. The hygrothermal sensors installed in each chamber were connected to a data acquisition device (P/N: OMB-DAQ-2416-4AO, OMEGA Engineering®, U.S) to measure the output voltages corresponding to temperature and relative humidity readings. The data collection interval was set to 60 seconds.

Images of the nylon porous membranes were captured using a Nikon D90 camera equipped with a macro lens (AF Micro Nikkor, Focal length: 60 mm, Aperture: 32 mm) directly pointing at the membrane, which was back-illuminated by a LED light (see Figure 1). Image analysis of the Gore-Tex membrane was not possible due to its dense multi-layered nature obfuscating any back illumination. For the nylon membrane, the captured raw images were converted to grayscale and binarized with darker cells (pores filled with liquid and the membrane itself) set to 0 (black). Lighter pixels (empty pores) were set to 1 (white). From the binarized image, the breathable area of the membrane was calculated.

Data collection, processing, and analysis methodology. The mass flow rate of moisture ($\dot{m}_v$) into the dry chamber of volume (V_d) through a piece of fabric is a function of the area of the membrane (A) and the difference in moisture concentrations between the two chambers ($C_{v,m}$ in the moist and $C_{v,d}$ in the dry chamber), which is given by

$$\dot{m}_v = V_d \, \dot{C}_{v,d} = KA(C_{v,m} - C_{v,d}) \tag{1}$$

where $\dot{C}_{v,d}$ is the rate of change of moisture concentration. The moisture diffusion coefficient (K) is the inverse of the transmission resistance [18] and depends on the membrane porosity (ϕ), thickness (L), and vapour diffusivity in air (D) [21,22].

Equation (1) can be rearranged to give the diffusion coefficient as a function of the instantaneous rate of change of moisture concentration and the difference in moisture concentrations of the two chambers, as given by equation (2). The rate of change in moisture concentration of the initially dry chamber ($\dot{C}_{v,d}$) is obtained by differentiating the line best fitting the moisture concentration profile (see Figure 4) with respect to time

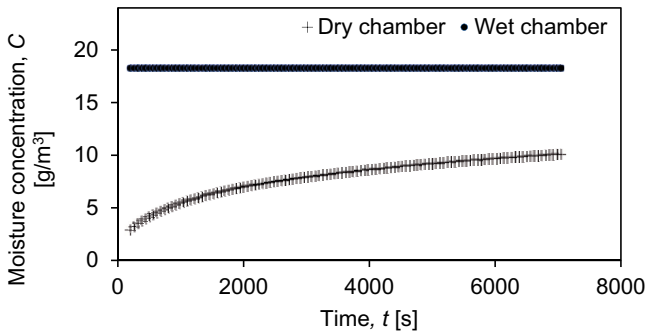$$K = \frac{\dot{C}_{v,d} V_d}{A \; (C_{v,m} - C_{v,d})} \tag{2}$$

Figure 4. Moisture concentration variation in both chambers is plotted as a function of time during a test of water vapour diffusion from the wet chamber to the dry chamber through a dry, clean nylon mesh.

Equation (2) can be discretized into a form suitable for calculating K from experimental measurements of vapour concentration at time intervals Δt

$$K \cong \frac{V_d\left((C_{v,d})_{t+\Delta t} - (C_{v,d})_t\right)}{A.\Delta t\ (C_{v,m} - C_{v,d})_t} \tag{3}$$

A psychrometric function was used to convert experimentally measured temperature and relative humidity readings into moisture concentration values for both the moist and dry chambers ($C_{v,m}$ and $C_{v,d}$) [23]. Figure 4 shows the moisture concentration variation with time for both wet and dry chambers in a nylon membrane permeation test. The two chambers were supplied with moist and dry air, respectively, until the wet chamber reached a relative humidity of above 95% and the dry chamber had a relative humidity of about 10% prior to the vapour diffusion experiments. These initial relative humidity values were selected as they were the highest and lowest that could be achieved repeatably with the experimental apparatus used. The moist chamber concentration remains constant, while the dry chamber increases with time as vapour diffuses through the membrane. The temperature gradient between the two chambers was negligible, and the wall temperatures were in equilibrium with the external and internal ambient air.

Two separate methods were used to calculate K. In the first approach; a logarithmic function was fit through the data for ($C_{v,d}(t)$) in Figure 4 and differentiated with respect to time in order to yield the rate of change of moisture concentration ($\dot{C}_{v,d}(t)$). These functions were then substituted into equation (2) to calculate the moisture diffusion coefficient as a function of the difference in moisture concentrations. Alternatively, the data for $C_{v,d}(t)$ was substituted in equation (3) at time intervals of $\Delta t = 60\,\text{s}$, and K was calculated. Figure 5 shows the values of K calculated using these two different methods as a function of the concentration difference ($\Delta C = C_{v,m} - C_{v,d}$) between the two chambers.
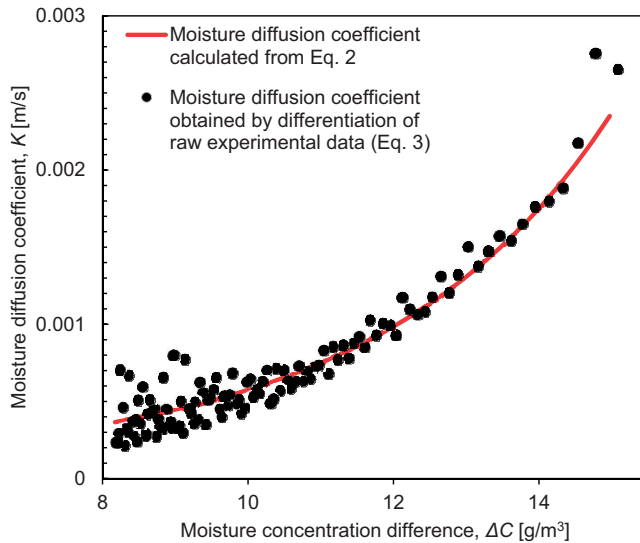
Figure 5. Moisture diffusion coefficient of the dry nylon membrane plotted against concentration difference between the chambers calculated using equation (2), shown by the solid line, and equation (3), shown by scattered data points.

The continuous line in Figure 5 was calculated using equation (2), while the data points were determined using equation (3). The data points show some scatter, especially at low concentration differences, since numerical differentiation magnifies variations in experimental measurements. Good agreement between the two data sets is observed. All further calculations of moisture diffusion coefficients presented in this research are determined using equation (2).

Repeatability and uncertainty analysis

Three experiments with similar initial conditions were performed on the microporous nylon membrane to investigate experimental repeatability. The relative discrepancy was obtained as the ratio of the standard deviation of moisture concentrations in the dry chamber at a given time to the mean value of moisture concentration. It was observed that the discrepancy remained <5%. To test the reliability of moisture diffusion coefficient analysis, the root mean square error of the exponential fit (see Figure 4) was obtained as 1.091×10^{-4} m/s. This translates to an average uncertainty of 4.1% in the measured diffusion coefficient when the moisture concentration difference is about $15 \, \text{g/m}^3$ and an average uncertainty of 20.8% when the moisture concentration is as low as $9 \, \text{g/m}^3$. As the difference in concentration between the two chambers decreases, the uncertainty increases as the numerator of equation (3) decreases. This can be countered by reducing the

sampling frequency so that data is acquired over a larger time interval. However, this reduces the time resolution of measurements. A sampling interval of 60 s was set to satisfy these conditions. The data used in the subsequent analysis was taken when the concentration difference was greater than 13 g/m^3, where the uncertainty was <5%.

Results and discussion

Dry nylon mesh and non-evaporative liquid contamination

The calculated vapour diffusion coefficient (K) of a dry nylon membrane at room temperature is a function of the moisture concentration difference (ΔC) across it, as shown by the curve (solid red line) in Figure 5. The variation can be described by an exponential function

$$K = 3.741 \times 10^{-5} \, e^{0.2877 \, \Delta C} \tag{4}$$

where the units of ΔC are g/m^3 and those of K m/s. This value of moisture permeability was calculated from experiments performed on a clean, dry nylon filter (see Figure 3(a)).

To investigate the impact of pore blockage on the porous membrane, a small droplet of glycerin was placed on the nylon membrane. A sample processed image of the porous membrane is shown in Figure 6(a), where the white dots represent open pores, and black spaces denote the porous membrane fibres or glycerin blockage. Glycerin was chosen because it is a safe chemical to work with that does not evaporate significantly at room temperature [24] and has high viscosity so that it remains where it is placed. The blocking part of the membrane should not change the value of K (which is defined per unit area of the breathable membrane) but reduces the open area (A) for vapour transmission in equation (1). The blockage area was varied from 8% to 78% by varying the amount of glycerin deposited. Measurements of humidity levels in the two chambers were used, following the procedure described above and equation (2), to determine the vapour diffusion coefficient values. Four different sets of tests were done in which the amount of blockage was progressively increased (8%, 21%, 43%, and 78% of the open membrane area), reducing A in equation (3) by corresponding amounts. Moisture diffusion coefficients for all four experiments, calculated at vapour concentration differences (ΔC) of 10 g/m^3, 12 g/m^3, 14 g/m^3, and 16 g/m^3, are plotted in Figure 7. The variation in calculated values for K is within the experimental uncertainty.

Water condensation and liquid water obstruction of nylon mesh filter

Water condensation on the porous membrane results in pore blockage and subsequently reduces the area open for vapour transmission. However, this liquid film can also evaporate from the membrane adding to the vapour to pass through the
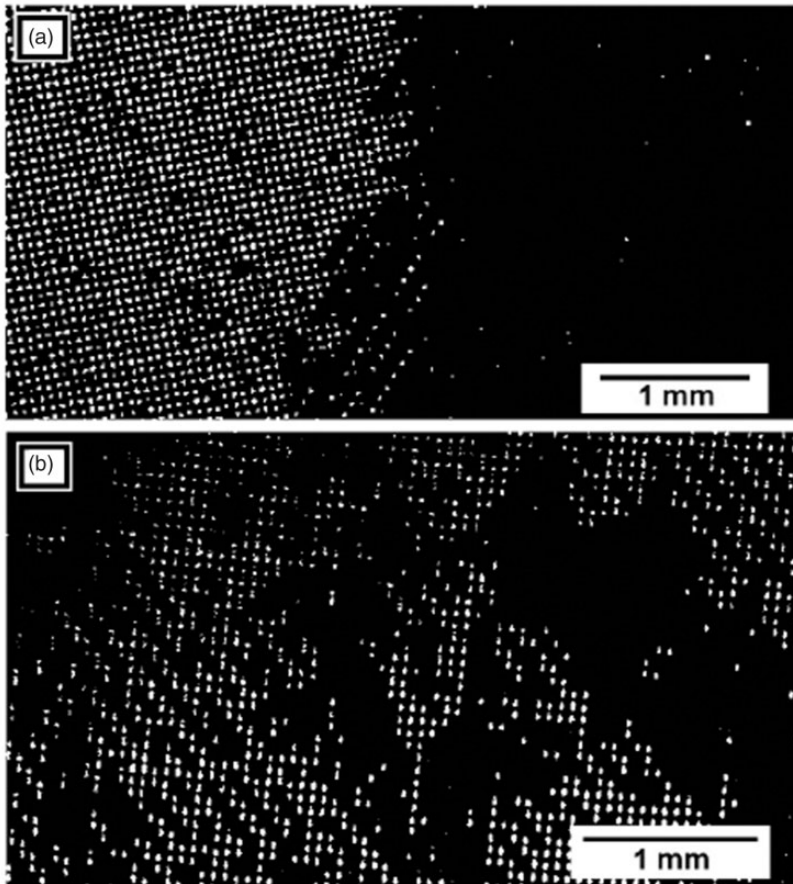
Figure 6. Processed images of the nylon mesh (a) partly contaminated by glycerin oil (b) with partial pore blockage due to the presence of condensed water on it.

membrane. To understand the effect of water blockage on moisture transmission, it is essential to separately quantify the contributions of water evaporating from the wet membrane and that which transfers through the porous membrane.

To investigate the water evaporation rate from the membrane, a small container of water with an open surface area of 94 mm^2 and depth of approximately 5 mm was placed within the sealed test chamber with an initial temperature of 22°C and relative humidity of 29%. As the water evaporated, changes in relative humidity were recorded and used to calculate vapour concentration. The increase in vapour concentration as a function of time is shown in Figure 8.

The experimental results were compared with the model of Boelter et al. [25], which predict that the evaporation rate (E [kg/hour]) from the surface of a
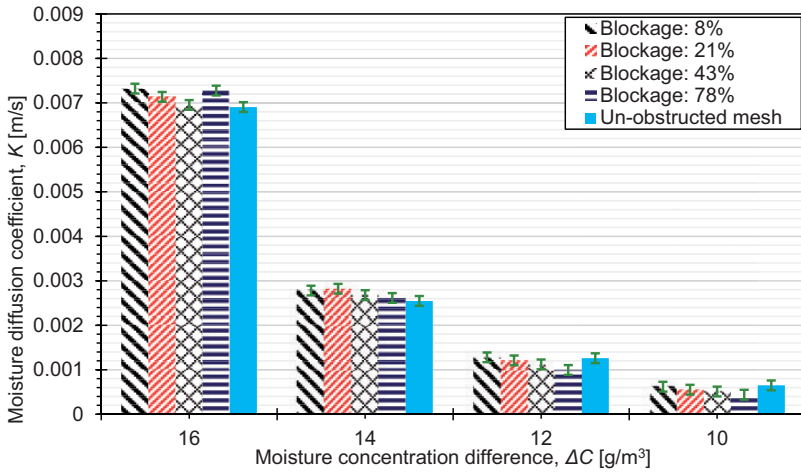
Figure 7. Moisture diffusion coefficient of nylon membrane measured with varying amounts of pores blocked by glycerin (8%, 21%, 43%, 78%), for moisture concentration differences of 10, 12, 14 and 16 g/m^3.
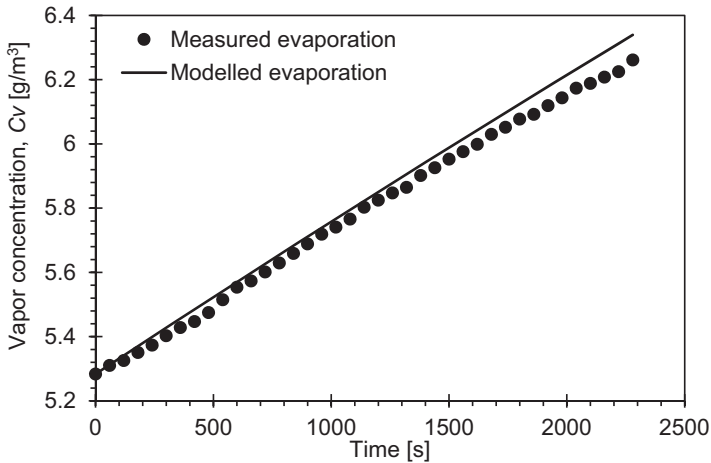

Figure 8. Change in vapour concentration due to film evaporation calculated from equation (5) (solid line), compared with experimental measurements (data points).

liquid layer, in the absence of any convective flows in the air surrounding it is given by
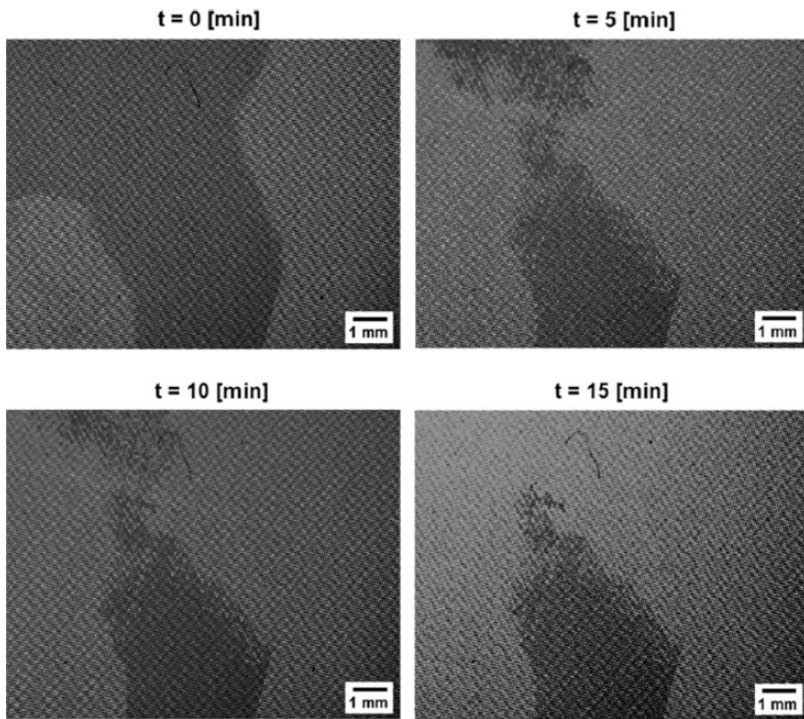
$$E = 0.0000162 A_w (P_{v,sat} - P_v)^{1.22} \tag{5}$$

Figure 9. Photographs of a section of the partially wet nylon membrane during test at $t = 0$, 5, 10, and 15 min.

where P_v is the partial pressure of water vapour at the surface of the liquid film, $P_{v,sat}$ the partial pressure at saturation conditions and A_w the surface area of the water film. The model's predictions are shown in Figure 8 (solid line) and show good agreement with experimental measurements with a maximum difference of 11%. Equation (5) was used to estimate the rate of evaporation from the surface of a wet membrane.

To simulate water condensation on the exposed membrane, warm moist air ($T \approx 47°C$, $R_h = 100\%$) from the bubble humidifier assembly was blown onto the membrane at room temperature ($T \approx 22°C$) from a distance of 5 cm for approximately 10 minutes shortly after the membrane was installed on the test apparatus. The membrane was allowed to cool to room temperature before vapour diffusion experiments were started. Figure 6(b) shows a processed binarised image of the nylon membrane with pores partially blocked by condensed water.

As the experiment proceeded, the water on the membrane evaporated so that the number of pores blocked by water decreased. Figure 9 shows photographs taken at 5 min intervals of a portion of the nylon membrane, with the darker regions revealing wet sections where pores were blocked. As the water evaporated,
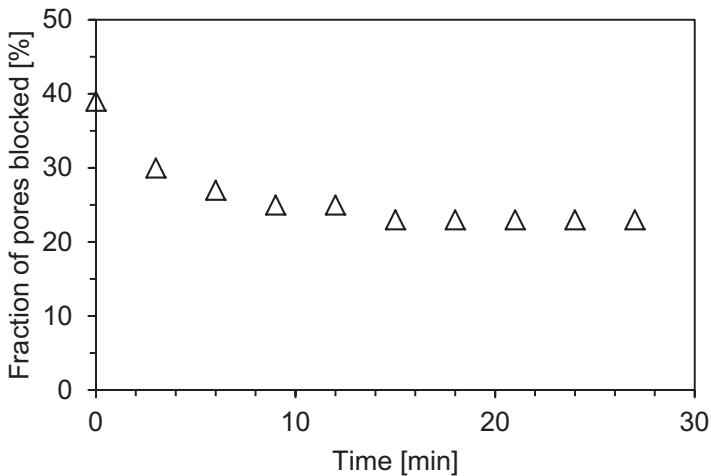
Figure 10. Fraction of pores in nylon membrane blocked by water as a function of time. Pore blockage tends to shrink due to the evaporation of water from the wet surface of the porous fabric.

the dark area decreased as more pores became open. Figure 10 shows the variation with time of the fraction of pores in the membrane blocked by water, measured at 3-minute intervals. Initially, 39% of the pores were blocked, but this decreased to 23% after 15 min and then stayed constant at this value.

Figure 11 shows the measured rate of change of moisture concentration in the initially dry chamber as a function of the difference in moisture concentration between the two chambers separated by an initially wet membrane. Included is the predicted rate of change (solid line) using the value of K from equation (4) and the open pore area determined from Figure 10. The predicted values are less than those measured, with a growing difference between the two as the moisture concentration difference increases. The additional moisture detected can be attributed to the evaporation from the surface of the membrane.

To estimate the rate of water evaporation from the surface of the membrane, it is necessary to know the wetted area A_w. The number of pores filled with water can be identified from photographs (see Figure 6(b)). However, it is not possible to know whether the liquid is confined to the pores or whether the surface of the mesh is also wetted. The wetted area was therefore assumed to lie between two bounds, $A_{w,min} < A_w < A_{w,max}$, as illustrated in Figure 12. The upper bound, $A_{w,max}$, was calculated assuming that half the width of the mesh around each pore filled with water was covered by a film of water (shown by the square marked in Figure 12(a) surrounding the four pores filled with water). The lower bound, $A_{w,min}$, assumed that the water was confined to the interior of the pores and did not wet the surrounding mesh (shown by the four small squares in Figure 12(b)). In reality,
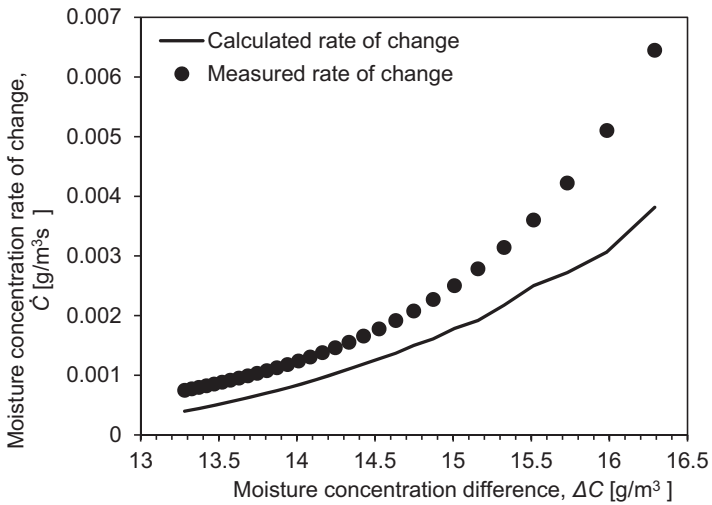
Figure 11. Expected vapour permeation rate plotted against moisture concentration difference compared with the measured rate of change of moisture concentration within the initially dry chamber.
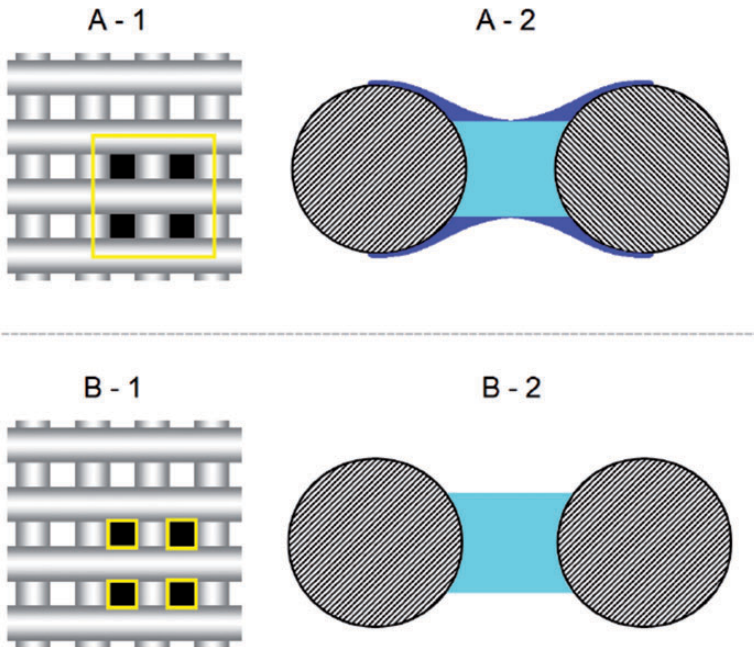

Figure 12. (A-1) Assumed wetted area used to model evaporation (upper bound) contains the pore area and the surrounding mesh. (A-2) Schematic cross-sectional representation of the wetted filter, showing that the fibre's surface is wet as well as the filled pore. (B-1) Assumed wetted area used to model evaporation (lower bound) only containing the blocked pores. (B-2) Schematic cross-sectional view of the wet pore, area of which was used for evaporation modelling.
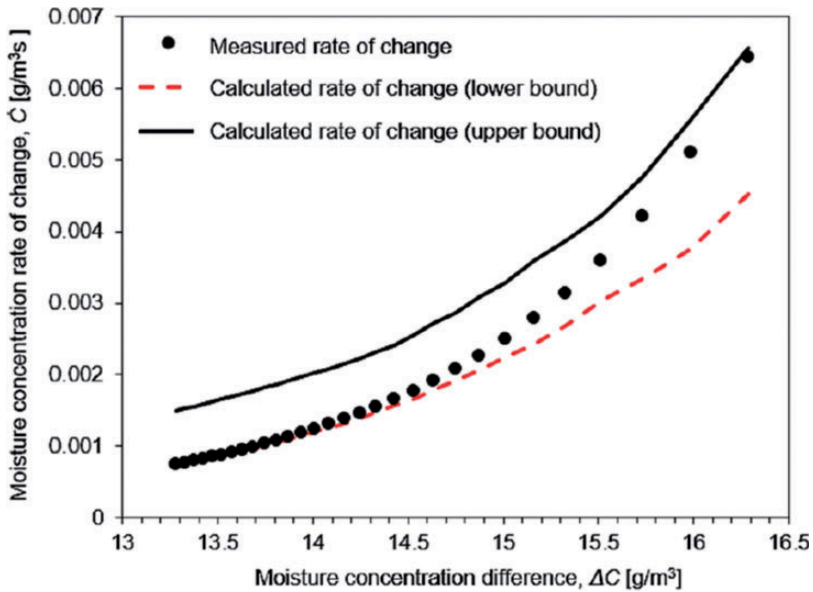
Figure 13. The measured rate of change of moisture concentration compared to the modelled rate of change of moisture concentration as a function of the difference in moisture concentration between the two chambers separated by a wet nylon membrane. The total modelled rate of moisture concentration combines the estimated permeation with the modelled evaporation. The upper bound model uses $A_{w,max}$ while the lower bound uses $A_{w,min}$ to estimate the moisture gain from evaporation.

it is likely that A_w decreased from $A_{w,max}$ to $A_{w,min}$ as the thin film on the mesh evaporated before the much thicker layer of water filling the pores.

The total amount of water evaporated from the surface of the film was calculated using either $A_{w,max}$ or $A_{w,min}$ in place of A_w in equation (5). This was added to the calculated rate of water vapour permeating through the membrane, shown in Figure 11. The result was two different estimates of the rate of change of moisture concentration in the dry chamber that represented the upper and lower bounds of predictions from the model. These are shown by lines in Figure 13, along with the experimental measurements. At high values of ΔC, which corresponded to the early stages of the experiment when the membrane was covered with condensed water, the data was close to the upper bound of predictions that assumed the mesh of the nylon membrane was wet. At low values of ΔC, which represent later times in the experiments, the lower bound estimates agreed well with experimental measurements. At intermediate values of ΔC, the measurements lay between these two bounds, supporting the hypothesis that initially, the rate of increase in moisture concentration was high due to evaporation from the surface of the mesh. Then as this dried out, the total evaporation rate decreased.
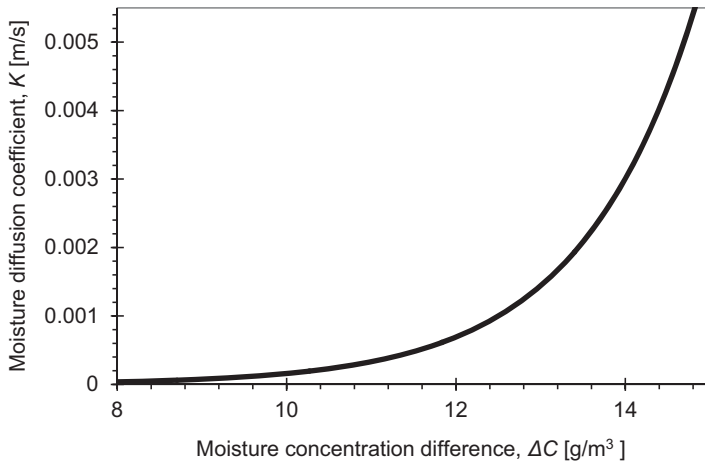
Figure 14. Moisture diffusion coefficient of dry Gore-Tex membrane plotted as a function of moisture concentration difference of either side of the membrane.

Water condensation and liquid water obstruction of Gore-Tex membrane

The moisture transmissivity coefficients of Gore-Tex membranes were characterized for three cases; initially dry and those exposed to a warm water mist for either 40 or 120 minutes prior to testing. The test procedure was identical to that followed for the nylon membrane, except that it was not possible to image water condensation on the Gore-Tex membrane due to its multi-layered dense structure (see Figure 3(b)) did not allow for light to pass through it. The open area for vapour diffusion was therefore not measured.

Figure 14 shows the vapour diffusion coefficient (K) of the dry Gore-Tex membrane as a function of the moisture concentration difference. When $\Delta C < 8\,\mathrm{g/m^3}$ K approaches zero, showing that there is negligible diffusion of vapour through the Gore-Tex membrane. This behaviour is different from that of the nylon membrane, which allowed significant diffusion through it even at low values of ΔC (see Figure 6). At more substantial moisture concentration differences ($\Delta C > 12\,\mathrm{g/m^3}$), values of K were higher than those of nylon. From this data, the moisture diffusion coefficient (K) through the Gore-Tex membrane for a given moisture concentration difference (ΔC) across it can be approximated by

$$K = 1.031 \times 10^{-7}\ e^{0.7343\ \Delta C} \tag{6}$$

Prolonged exposure to a heated flow of moist air prior to testing significantly reduced vapour diffusion through the Gore-Tex membrane. Figure 15 shows the rate of increase in moisture concentration in the dry chamber as a function of moisture concentration difference for a dry membrane and those that had been
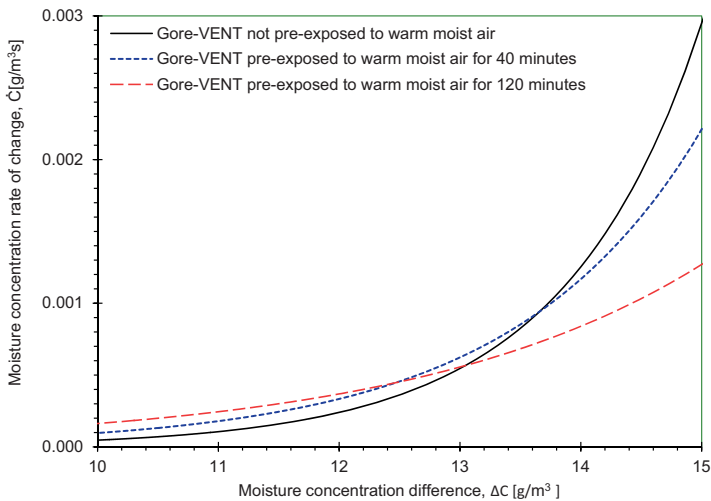
Figure 15. The measured rate of change of moisture concentration in the initially dry chamber as a function of the difference in moisture concentration between the two chambers separated by a Gore-Tex membrane (Gore-VENT). Results are shown for an initially dry membrane and those exposed to warm, moist air for 40 or 120 min prior to the start of the test.

exposed to a warm water mist for 40 min and 120 min, respectively. For ΔC >13.5 g/m³, the dry membrane had the highest vapour diffusion rate, whereas those exposed to moisture had lower diffusion rates. It is plausible that the pores in the membrane were blocked by condensed water, which prevented vapour diffusion. The diffusion of water through the membrane exposed to the mist for 120 min was much lower than that exposed for 40 min.

At low concentration differences (ΔC <13.5 g/m³), the moisture concentration rate to the dry chamber was slightly greater for the pre-wetted membranes than the dry membrane. This may be due to evaporation from the surface of the membranes rather than diffusion through them. Since the diffusion rate is low at lower values of ΔC, water evaporating from the surface of the membrane may be a significant portion of the moisture entering the dry chamber.

Conclusions

This research investigated the rate of water vapour transmission through microporous nylon and nanofibrous Gore-Tex membranes. The mass flow rate of water vapour diffusing through a porous membrane is shown to be proportional to both its area and the difference in vapour concentration across its two faces, such that $\dot{m}_v = KA\Delta C$. An exponential relationship is observed between the moisture diffusion coefficient (K) and the moisture concentration difference (ΔC) between the high and low humidity environments is shown for the nylon membrane. Contamination of the membrane by a non-volatile liquid is shown to decrease

the rate of moisture diffusion through the porous membrane due to pore blockage and the subsequent reduced porous membrane open area. Prolonged exposure to moist air is noted to result in condensation of water on the porous membrane, blocking pores and decreasing its effective open area, reducing the vapour diffusion rate through it. Water within and on the porous membrane is also observed to increase the mass of water vapour transferred into the low humidity environment through evaporation. The total amount of water vapour penetrating the nylon membrane was modelled and accounted for water vapour diffusing through and water evaporating from the membrane. The model was shown to have good agreement with the experimental data.

At low vapour concentration differences ($\Delta C < 8 \, \text{g/m}^3$), negligible water vapour diffusion through the Gore-Tex membrane was observed. Similar to the nylon membrane, an exponential relationship is observed between the moisture diffusion coefficient (K) and the moisture concentration difference (ΔC) the high and low humidity environments. For the Gore-Tex membrane, at $\Delta C > 12 \, \text{g/m}^3$, K is observed to be larger its nylon counterpart under similar ΔC conditions. The rate of vapour diffusion through the Gore-Tex membranes decreases when exposed for extended time periods to moist, warm air due to vapour condensation to the porous membrane.

Declaration of conflicting interests

Funding

ORCID iDs

Ariana Khakpour (iD) https://orcid.org/0000-0003-1553-2002
Michael Gibbons (iD) https://orcid.org/0000-0002-2668-1954

References

[1] Mal P, Ghosh A, Majumdar A, et al. Engineering of knitted cotton fabrics for optimum comfort in a hot climate. *F&Tinee* 2016; 24: 102–106. doi: 10.5604/12303666.1191434

[2] Fridrichová L, Frydrych M, Herclík M, et al. Nanofibrous membrane as a moisture barrier. In: *The 3rd joint international conference on energy engineering and smart materials (ICEESM-2018)*, 22-24 June 2018, Milan, Italy. DOI: 10.1063/1.505110

[3] Gore WL and Associates I. Venting: automotive, packaging, protective & portable electronics vents, 2020, https://www.gore.com/products/categories/venting?view=protective-vents-for-outdoor-electronics (accessed 14 May 2020).

[4] Laukkarinen A, Kero P and Vinha J. Condensation at the exterior surface of windows. *J Build Eng* 2018; 19: 592–601.

[5] El Diasty R and Budaiwi I. External condensation on windows. *Construct Build Mater* 1989; 3: 135–139. DOI: 10.1016/0950-0618(89)90004-4

[6] Perrotta A, García SJ and Creatore M. Ellipsometric porosimetry and electrochemical impedance spectroscopy characterization for moisture permeation barrier layers. *Plasma Process Polym* 2015; 12: 968–979.

[7] Zhang X, Yang X and Chase GG. Filtration performance of electrospun acrylonitrile-butadiene elastic fiber mats in solid aerosol filtration. *Sep Purif Technol* 2017; 186: 96–105.

[8] Chaney DR, Demars K, Eischens G, et al. Proposed standard test method for measurement of pneumatic permeability of partially saturated porous materials by flowing air. *Geotech Test J* 1996; 19: 232.

[9] Barucci M, Bianchini G, Del Rosso T, et al. Thermal expansion and thermal conductivity of glass-fibre reinforced nylon at low temperature. *Cryogenics* 2000; 40: 465–467.

[10] Vaze J and Chiew FHS. Experimental study of pollutant accumulation on an urban road surface. *Urban Water* 2002; 4: 379–389.

[11] Alotoom A. Prediction of the collection efficiency, the porosity, and the pressure drop across filter cakes in particulate air filtration. *Atmos Environ* 2005; 39: 51–57.

[12] Fan J and Keighley J. The design of effective clothing for use in windy conditions. *Int J Clothing Sci Technol* 1989; 1: 28–32.

[13] Min J, Hu T and Liu X. Evaluation of moisture diffusivities in various membranes. *J Membr Sci* 2010; 357: 185–191.

[14] Das S and Kothari VK. Moisture vapour transmission behaviour of cotton fabrics. *Indian J Fibre Text Res* 2012; 37: 151–156.

[15] Rossi RM, Gross R and May H. Water vapor transfer and condensation effects in multilayer textile combinations. *Text Res J* 2004; 74: 1–6.

[16] Ren YJ and Ruckman JE. Water vapour transfer in wet waterproof breathable fabrics. *J Ind Text* 2003; 32: 165–175.

[17] Choudhary MK, Karki KC and Patankar SV. Mathematical modeling of heat transfer, condensation, and capillary flow in porous insulation on a cold pipe. *Int J Heat Mass Transfer* 2004; 47: 5629–5638.

[18] Farnworth B, Lotens WA and Wittgen P. Variation of water vapour resistance of microporous and hydrophilic films with relative humidity. *Text Res J* 1990; 60: 50–53.

[19] McMaster C (n.d.). Nylon plastic mesh 371 × 371 mesh size, 40″ wide, https://www.mcmaster.com/9318T25/ (accessed 15 February 2021).

[20] Gore WL & Associates (2020) GORE® Protective vents – adhesive series – data sheet & installation guide, https://www.gore.com/system/files/2020-09/PTV-DataSheet-Adhesive-Series-EN-WEB.pdf (accessed 16 February 2021).

[21] Pan N and Gibson P. *Thermal and moisture transport in fibrous materials*. Boca Raton, FL: CRC Press, 2006.

[22] Cussler EL. *Diffusion: Mass transfer in fluid systems*. 2nd ed. New York, NY: Cambridge University Press, 1997.

[23] Kennedy HE, Amp and Owen MS. Psychometric charts. In *2009 ASHRAE handbook: fundamentals*. Atlanta, GA: American Society of Heating, Refrigeration, and Air-Conditioning Engineers, 2009.

[24] Glycerine Producers Assoc. Physical Properties of glycerine and its solutions. New York, NY: Glycerine Producers Assoc, 1975.

[25] Boelter LMK, Gordon HS and Griffin JR. Free evaporation into air of water from a free horizontal quiet surface. *Ind Eng Chem* 1946; 38: 596–600.

Appendix

Notation

A   area (m^2)
C   mass concentration (g/m^3)
$\dot{C}$ mass concentration rate of change (g/m^3 s)
D   vapour diffusion coefficient in air (m^2/s)
E   evaporation rate (kg/h)
K   moisture diffusion coefficient through a membrane (m/s)
L   thickness (m)
$\dot{m}$ mass flow rate (g/s)
P   pressure (Pa)
R_h relative humidity (%)
t   time (s)
T   temperature (°C)
V   volume (m^3)
ϕ porosity ($-$)

Subscript

d   dry chamber
l   liquid
m   moist chamber
sat   saturation state
v   vapour